Bending-related faulting and mantle serpentinization at the Middle America trench

C. R. Ranero[1], J. Phipps Morgan[1], K. McIntosh[2] & C. Reichert[3]

[1]GEOMAR and SFB574, Wischhofstrasse 1-3, 24148 Kiel, Germany
[2]Institute of Geophysics, University of Texas at Austin, 4412 Spicewood Springs Rd., Bldg 600, Austin, Texas 78759-8500, USA
[3]BGR, Bundesanstalt für Geowissenschaften and Rohstoffe, Stilleweg 2, 30655 Hannover, Germany

The dehydration of subducting oceanic crust and upper mantle has been inferred both to promote the partial melting leading to arc magmatism and to induce intraslab intermediate-depth earthquakes, at depths of 50–300 km. Yet there is still no consensus about how slab hydration occurs or where and how much chemically bound water is stored within the crust and mantle of the incoming plate. Here we document that bending-related faulting of the incoming plate at the Middle America trench creates a pervasive tectonic fabric that cuts across the crust, penetrating deep into the mantle. Faulting is active across the entire ocean trench slope, promoting hydration of the cold crust and upper mantle surrounding these deep active faults. The along-strike length and depth of penetration of these faults are also similar to the dimensions of the rupture area of intermediate-depth earthquakes.

Since the proposition that intermediate-depth earthquakes occur by reactivation of outer rise faults[1], considerable discussion has concentrated on possible mechanisms that would allow seismogenic slip at these large confining pressures where plastic deformation would be anticipated[2]. A commonly invoked mechanism to promote brittle failure is the decrease in effective normal stress induced by increased pore pressure during dehydration reactions[3–6]. As oceanic plates dive into subduction zones, progressive metamorphism releases fluids chemically bound in the slab. Such fluid release, if concentrated along pre-existing fault weaknesses, may facilitate seismogenic slip across the upper part of the slab[4] or even tens of kilometres into the slab's mantle[7]. In Tonga, the similar orientation and dip (relative to the slab surface) of nodal planes of intraslab intermediate-depth seismicity and nodal planes of outer rise events has been interpreted to support this hypothesis[8]. Although bending-related normal faulting occurs at all subduction zones, little high-resolution data exists to permit testing of this hypothesis.

If slab-released fluids enter overlying asthenosphere, there they can induce 'wet' partial melting and the formation of magmatic arcs[9]. It has been realized that at some subduction zones, dehydration of most of the hydrous phases contained in subducting sediments and ocean crust should occur at shallower depths than the depths of magma generation—thus the fluids inducing arc-melting are likely to come from the slab's mantle[10]. However, the feasibility of large-scale hydration of the upper ocean mantle is still under debate[11], with different calculations of the global fluid budget entering subduction zones, assuming that water might be stored in the sediments and crust[12,13] or in the mantle[6]. Where most of the hydration of the incoming plate takes place also remains in doubt: near a spreading centre[4,10], intraplate by fluids rising from underlying mantle plumes[14], or beneath the outer rise, mainly in the crust[4], or perhaps also in the mantle[7]. At the outer rise, some earthquakes have been proposed to cut >20 km deep into the lithosphere[15,16], suggesting a possible pathway for sea water to reach and react with cold lithospheric mantle. (However, the typical hypocentral depths of outer rise earthquakes remains under debate.)

Here we present new evidence documenting that bending-related faulting at the trench offshore Nicaragua has created a pervasive extensional faulting system that cuts through the crust of this incoming plate, penetrating deeply into the lithospheric mantle. Faulting remains active across the entire ocean trench slope, promoting deep percolation of water and modification of the properties of the incoming ocean plate just before its subduction.

Relation between bend-faulting and seafloor spreading fabric

Multibeam bathymetry along the Middle America trench (MAT) shows that bending-related extensional faulting (bend-faulting) is pervasive across most of the ocean trench slope (Fig. 1). The crustal thickness and the orientation of the tectonic fabric formed at the spreading centre seem to govern the amount of faulting and trench depth for each of the four tectonic segments within Fig. 1. Along this margin, the age of the subducting lithosphere most probably has a secondary role as it changes little and gradually along the incoming plate—lithosphere formed at the Galapagos spreading centre (segments 1–3) ranges from ~14 Myr off South Costa Rica to ~22 Myr off the middle of the Nicoya peninsula, while lithosphere formed along the East Pacific Rise (segment 4) is 24 Myr along the Nicaragua trench[17]. Segments with the most pervasive faulting and larger offsets (segments 2 and 4 in Fig. 1) are associated with 5–7-km-thick crust and magnetic anomalies striking at low angles to the trench.

This indicates that, for lithosphere of the same age, bend-faults develop best when they reactivate faults formed at the palaeospreading centre, which occurs when the strike of the inherited tectonic fabric is nearly parallel to the axis of bending of the incoming plate. Feedback between faulting and flexure is inferred from the structures: faults are initially reactivated owing to bending, but trench parallel faulting appears to lead to larger bending and to the development of new faults, in spite of a similar 'elastic thickness' across much of the margin. This is best seen by comparing the ocean plate facing the Nicoya peninsula and Nicaragua, where the age and crustal thickness are essentially the same, but the number of faults and their offsets are larger to the north, where bending is also larger.

Similarly, the plate at segment 2 bends more than at segment 3, where magnetic anomalies strike perpendicular to the trench. The subducted slab steepens gradually to the north from 35–45° beneath Costa Rica to ~65° beneath Nicaragua[18], implying increasing net plate bending towards the North. We concentrate our analysis on segment 4 (Fig. 1), which shares the morphologic characteristics of

many circumpacific subduction zones in regions without oceanic plateau and spreading-centre subduction (for example, Peru and Chile trench[19–21]; Japan-Kuril trench[22]; the Tonga-Kermadec, Aleutian and Java trenches[23]).

Seismic images of bend-faulting

Multichannel seismic (MCS) reflection images across the oceanic trench slope show two main sets of reflections beneath the sediments. A set of subhorizontal reflections occurs ~1.7 s beneath the top basement delineating the base of the crust (Fig. 2a, b). A second set appears as trenchward-dipping reflections across the crust and mantle. Some dipping events traverse the ~5.5-km-thick crust and align with reflections in the mantle which extend at least to depths of 18–20 km beneath the sea floor. Deeper than 18–22 km, reflections are obscured by the energy of the water-layer multiple so that their ultimate depth is unconstrained. Locally, there are also seaward-dipping reflections in the mantle (Fig. 2a), although this reflectivity is notably less pervasive than the landward-dipping fabric. The seismic profiles shown in Fig. 2a and b were shot in opposite directions, normal to the seafloor topography, indicating that neither the reflections nor their dominant dipping direction are artefacts of the data acquisition and processing[24].

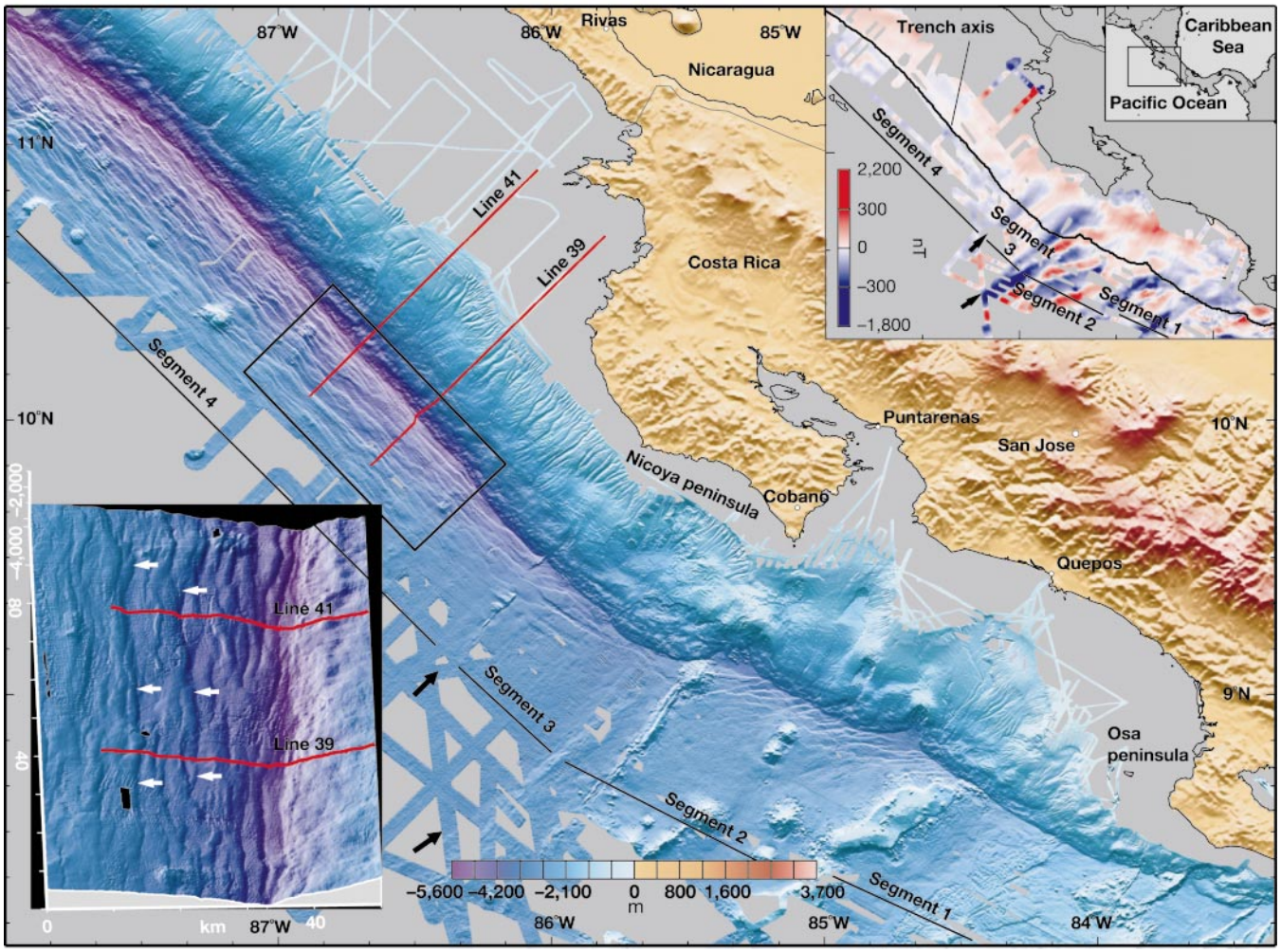

Figure 1 Colour-coded bathymetry and elevation map along ~600 km of the Middle America trench. Bathymetric soundings have been edited before gridding into a ~100 m grid spacing. Land topography is from a 30-arcsecond data base from US geological survey. Red lines are tracks from seismic profiles in Fig. 2. The data display the deformation of the ocean plate related to bending before subduction. Abrupt boundaries separate four distinctly faulted segments of the ocean plate[17,47] (black arrows mark segment boundaries). Segment 1 is off southern Costa Rica, where the 12–20-km-thick crust of the Cocos ridge bends little, and little to no fault relief develops near the trench. The large fault scarps perpendicular to the trench predate sediment infill, indicating that they formed ~14 Myr ago when the Galapagos hotspot affected this area and are not related to subduction. Segment 2 has ~7-km-thick crust and magnetic anomalies striking oblique to the trench. Here pervasive faulting with a strike similar to the original seafloor fabric develops within ~25 km of the trench axis. Segment 3 has ~6-km-thick crust, a smooth morphology and magnetic anomalies striking perpendicular to the trench axis. In segment 3, a few small-offset faults develop, roughly parallel to the trench and at high angles with the inherited tectonic fabric. Here the plate bends less than at contiguous segments and little deepening occurs towards the trench axis. A small linear scarp in the ocean plate separates segments 3 and 4. Lithosphere to the SE (segments 1 to 3) formed at the Galapagos spreading centre (see upper inset), whereas lithosphere to the NW (segment 4) formed at the East Pacific Rise. Although the lithosphere of segments 2 to 4 formed at similar spreading rates, major changes in plate bending and faulting occur. Segment 4 has 5–6-km-thick crust, magnetic anomalies striking parallel to the trench and pervasive normal faulting. The faulted region is the widest in this region, increasing towards the north from ~25 to ~60 km, while individual fault throws increase from ~100 to ~500 m. The two sets of white arrows in the lower inset mark seafloor offsets of two ~50-km-long faults; these faults are imaged as clear deep penetrating faults in the seismic sections (Fig. 2). Lower inset shows a perspective close-up view of the bathymetry projected along the trench (100 × 50 km). Area is indicated by the box in regional figure and view is from SE. Upper inset shows a magnetic map of the area[17].

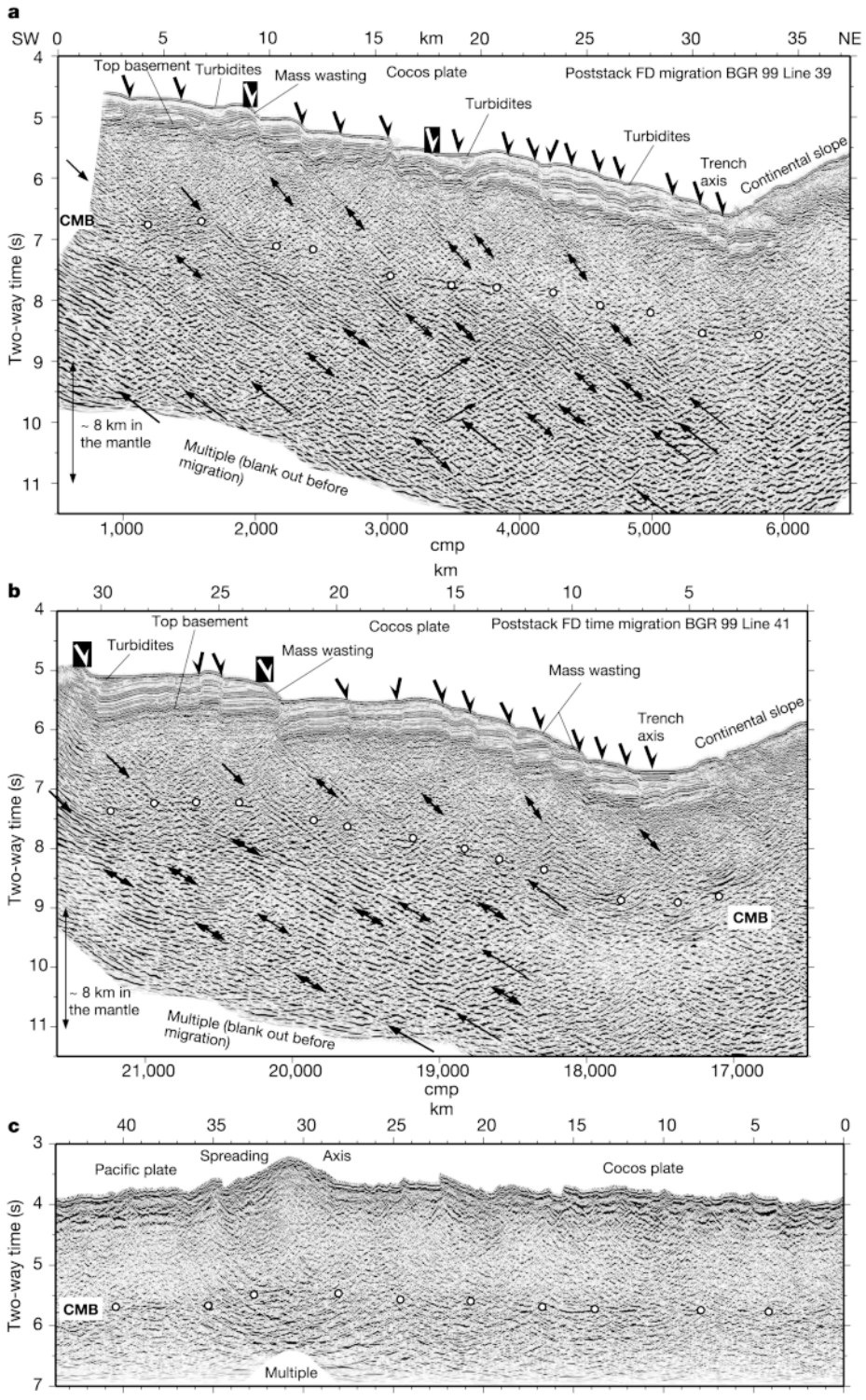

Figure 2 Poststack finite-difference time migration of various lines. **a**, Line 39 and **b**, line 41 of cruise BGR99 and **c**, line 1331 of Ewing cruise 9503. Lines 39 and 41 show the structure of the Cocos plate across the ocean trench slope. The crust–mantle boundary (CMB) is defined by a series of gently dipping reflections, delineated by white filled circles, at ~1.7 s two-way time (~5 km) beneath the top of the igneous basement. A pervasive fabric traverses the mantle: sometimes this fabric appears to continue up into reflections that cross the crust projecting into top-basement and seafloor offsets. Several reflections align forming individual features—indicated by the black arrows—that cross much of the lithosphere. We propose that these reflections represent normal faults which slip during plate bending. The reflections cut to ~18–20 km across the crust into the mantle where they are masked by the acoustic energy of the seafloor multiple. Arrows at the sea floor indicate faults used for Figs 3 and 4. Seafloor mass-wasting processes are evidenced by truncation of strata at many fault scarps and by turbidite infill of half-grabens. White arrows in black boxes indicate faults marked by arrows in the lower inset of Fig. 1. Line Ewing 9503-1331 shows the structure of the ocean plate formed at the East Pacific Rise at latitude 16° N (ref. 27). The crust–mantle boundary is defined by discontinuous reflections at ~1.8 s two-way time, the crust and upper mantle are featureless. The 'smiles' underneath the spreading centre axis are created by overmigration of side-scattered energy in the rough axial topography. FD, finite difference.

Trenchward-dipping reflections across the crust and mantle project updip to the largest offsets in top basement and sea floor, indicating that these represent reflections from fault planes. Fault offsets at the sea floor are <200 m—that generate <50 ms travel-time offsets at the Moho, which explains the lack of clear offsets across the crust–mantle boundary reflections. Although these faults appear to form by reactivation of faults created at the palaeospreading centre, such a deeply penetrating tectonic fabric could not have originated during crustal accretion at the palaeospreading centre. Modern MCS data collected over sea floor created at fast-spreading mid-ocean ridges (MOR) demonstrates that the reflective mantle fabric observed at the MAT was not formed by accretion/deformation processes at the fast-spreading East Pacific Rise (EPR).

Since the first modern MCS reflection survey was collected across the EPR at 9°–13° N, where the Cocos plate subducting beneath Middle America is formed, seismic images have shown a "reflection-free" mantle underlying the Moho reflection[25]. More recent MCS data, collected along segments of the EPR, comparable in quality to our near-trench data (for example, at 14°–18° S (ref. 26); and at 15.5°–16.5° N (ref. 27)), support earlier results (Fig. 2c). Seismic images of old crust formed at fast-spreading rates have regions of reflectivity limited to the crust and no evidence for crustal-scale brittle faulting[24]. Furthermore, theoretical modelling indicates that at the axis of fast-spreading MORs, the brittle layer overlying the persistent magma lens is only a few kilometres thick[28,29]. At the MAT, the strength of the mantle-dipping reflections is comparable to the Moho reflection (Fig. 2a, b), indicating that a similar fabric at the EPR would have been detected with seismic methods had it also existed there (Fig. 2c).

Further evidence against the origin of the reflective mantle fabric by ductile deformation at fast-spreading MORs comes from studies of ophiolite exposures. The ductile foliation of exposed mantle peridotites lies at a low angle to the Moho[30], a much shallower angle than the ~45° observed in the mantle reflections. These observations are also consistent with numerical models predicting that the mantle deformation fabric would lie semi-parallel to the Moho boundary[31].

Finally, data collected in the Cocos plate in the lithosphere halfway between the EPR crest and the Nicaraguan trench shows that reflectivity in the mantle is not produced during the ageing of the ocean plate as it drifts towards a subduction zone[32]. Dipping reflections observed in old lithosphere formed at other fast-spreading MORs are constricted to the lower crust[24]. Even in crust formed at slow-spreading rates, most seismically imaged normal faults are restricted to crustal levels[33], penetrating (rarely) at most a few kilometres across the Moho—again with a reflectivity pattern completely unlike that seen at the MAT.

At the MAT, dipping reflections appear to be images of deeply propagating faults formed by reactivation of shallow crustal faults created at the spreading centre. At fast-spreading MORs, roughly half the faults dip inward and half dip outward[34]. As lithosphere bends at trenches, faults can penetrate deeply into a 30–40-km-thick cold and brittle layer. During initial bending near the trench both inward and outward faults may be reactivated[23], which could explain the few and indistinct seaward-dipping reflections in the mantle. However, the seismic images and fault scarps in the bathymetry show that landward-dipping faults prevail both in the seafloor fabric of this particular ocean trench slope and in the reflective fabric of its underlying lithospheric mantle (Fig. 2a, b).

Offsets of individual faults measured at the sea floor and the top of the igneous crust show consistent differences: the top basement fault offsets are in most cases larger, with the difference increasing approaching the trench (Fig. 3). These differences, and the truncation of strata at the sea floor near fault scarps (Fig. 2), indicate that fault offset at the sea floor is often obscured by mass wasting, which tends to decrease surface fault relief. Indeed, small wedges of turbidites are observed at the foot of some fault scarps (Fig. 2). This may be the reason why a study at a different area[22] based upon

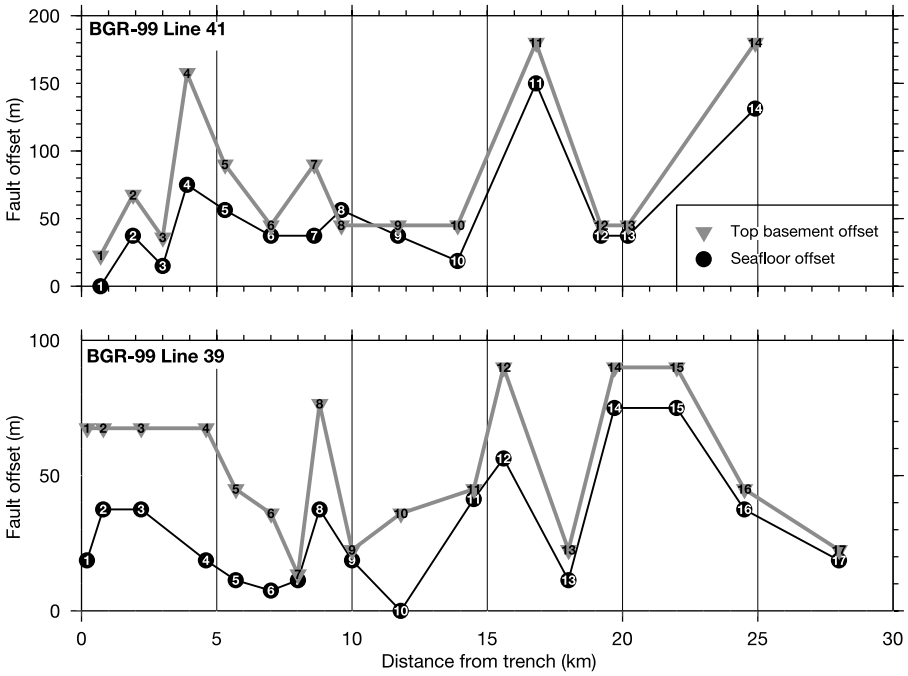

Figure 3 Fault offsets measured at the sea floor and top of igneous basement for faults marked on Fig. 2, plotted versus distance to the trench axis. The difference in fault offset at the sea floor and top basement is readily explained as a by-product of active mass-wasting processes that decrease the offsets of seafloor scarps. In this case, near-trench faults with similar seafloor and top basement offsets (for example, faults 7 and 9 at line 39 and faults 5, 7 and 8 at line 41) indicate recently formed faults, which typically have small offsets. Faults showing large differences in offsets (for example, faults 1–6 on line 39, and 3, 4 and 6 on line 41) would be faults formed away from the trench axis which continued to slip and experience surface mass-wasting as they approached the trench axis.

only bathymetric data suggested that active faulting stops in the middle of the trench slope. Here, the increase in the difference in fault offset between sea floor and top basement approaching the trench indicates that faulting remains active across the entire trench slope. Both the average fault offset and the number of faults increase towards the trench (Figs 3 and 4), implying both continued fault slip and fault formation in this region.

The observations can be explained with a model of sequential fault generation during progressive plate bending. First, widely spaced faults are reactivated during initial plate bending at the outer rise. Next, the segments between faults are cut by new faults as the plate approaches the trench axis and bending continues. Recent faults formed near the trench have similar fault offsets (see faults 6, 8 and 9 at line 41 and faults 7, 9 and 11 at line 39 in Fig. 3) at the sea floor and top basement, whereas older faults have a larger offset at the top basement than at the sea floor (see faults, 4, 5 and 7 on line 41 and faults 1–6 and 8 on line 39 in Fig. 3).

Where bend-faulting occurs, extension remains active across the entire oceanward trench slope, providing an environment where fluids can be persistently pumped down into the chemically reactive lithospheric mantle and crust. Offshore of Nicaragua, the thermal structure of the ~23-Myr-old plate implies that the brittle–ductile transition (~600 °C) is ~35 km deep; earthquakes may rupture to the mantle depths indicated by fault reflections. This scenario may promote pumping of water[35] across the crust into the mantle. At temperatures <500–600 °C mantle peridotite is unstable with respect to water and readily 'corrodes' to serpentinite. Serpentinization leads to important physical and chemical changes in the subducting lithosphere. It involves a large volume increase—complete serpentinization of a peridotite decreases its density by ~40%—promoting self-sealing closure of any open fluid conduits along faults. However, persistent brittle faulting across the entire trench slope may effectively reopen and recreate pathways for intensive fluid transport into the lithosphere.

The seismic data images a series of discrete reflections across the ocean crust and a more pervasive tectonic fabric beneath the crust–mantle boundary (CMB) (Figs 2a, b). Some of the most conspicuous dipping reflections in the mantle do not extend up into crustal reflections, while in other cases bright mantle reflections project updip into indistinct crustal reflections. We suggest that serpentinization (and perhaps also free fluids) produces the bright mantle reflectivity; the small offsets along observed faults would not be enough to create an anisotropic fabric detectable by seismic reflection methods. The more pervasive reflection fabric of the mantle does not necessarily indicate that the deformation between crust and mantle is decoupled but rather that tectonic structures in the mantle are easier to detect because mantle peridotites hydrate more easily and extensively than basaltic ocean crust.

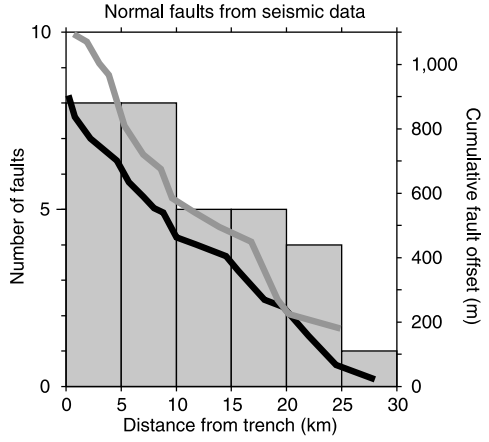

Figure 4 Histogram of fault density versus distance to the trench axis. The number of faults increases towards the axis, indicating that new faults continue to form as the plate approaches the trench axis. Lines indicate the cumulative fault offset measured at top basement for line BGR99-39 (black line) and BGR99-41 (grey line). There is a tendency to larger fault offset towards the trench.

The spacing in between packages of reflections defining faults in the mantle is somewhat shorter than between fault scarps at the sea floor (Fig. 2). A possible explanation is that at mantle depths where velocities are close to 8 km s^{-1}, the dominant frequencies of the returned signal (10–15 Hz) are lower than in the signal coming from the sediment section (45–80 Hz), so the deep portion of the faults may image as a broader area. Also, the Fresnel zone, that is, the dimensions of the lateral area sampled by the seismic wavefield, is broader for long travel times and thus the image of mantle reflectors is not as sharp as for shallow faults because the seismics are mapping a three-dimensional (3D) structure onto a two-dimensional cross-section. Furthermore, fault zones usually broaden as they deepen, so that the faults we observe may not be simple planes but rather packages of fractures. At the sea floor, arrays of faults arrange in longer fault segments (Fig. 1, lower inset). If faults broaden into the crust and mantle, fracturing may affect a larger volume at depth than at the sea surface.

The observed 50-km-wide region of pervasive faulting offshore of Nicaragua between the onset of faulting and the trench axis (Fig. 1) implies, at current convergence rates, that extension and water percolation have occurred there for at least 0.7 Myr. This time span is similar to the time that ocean lithosphere faults at slow-spreading MORs, but offshore of Nicaragua the water can penetrate at least four times deeper into the mantle before reaching the 600 °C isotherm. The incoming ocean lithosphere along the circumpacific subduction zones was almost entirely formed at intermediate- to fast-spreading MORs where axial faulting and associated vigorous hydrothermal circulation is believed to be shallower (~2–3 km depth) than typical at slow-spreading centres (~8–10 km depth). Thus bend-faulting, in addition to hydrating the mantle, may lead to pervasive pre-subduction hydration of crust formed at fast-spreading MORs, perhaps comparable to the crustal hydration experienced at slow-spreading MORs.

Faulting and intraslab seismicity

Faults in the seismic data dip ~45° and cut to at least 20 km into the plate (Fig. 2). Similarly, nodal planes of outer rise earthquakes elsewhere dip ~40–45° (refs 15, 36). More controversial is the proposition that earthquake rupture depths extend to ≥20 km (for example, ref. 36). The depth of penetration of faulting seismically imaged here supports the hypothesis that earthquakes can cut down at least 20 km beneath the sea floor.

The combination of swath bathymetry and seismic data provides insights into the 3D structure and dimensions of bend-faults. Some faults imaged on both seismic lines project updip to the same fault scarp at the sea floor. Two examples of deep penetrating faults are marked in Fig. 2 with white arrows. These faults cut the sea floor at the scarps marked with white arrows in the lower inset of Fig. 1—scarps which extend for 50 km or more. Thus individual fault planes can be ~50 km long along strike by ~20 km deep into the plate—dimensions similar to, or somewhat larger, than the size of the rupture area of individual intermediate depth earthquakes[5].

The reflectivity of the small-offset, deep-penetrating faults imaged in the seismic data can be best explained by water percolation and mineral alteration along the fault planes. Support for robust hydrothermal circulation associated with bend-faulting comes from the low heatflow values measured at the trench off Costa Rica[37] and elsewhere[38]. Thus serpentinized bend-faults may become regions where increased relative concentrations of hydrous minerals promote rupture of a fault several times during its descent. Crustal sections should generally dehydrate at shallower depths than mantle sections, in part because of the lower pressure/temperature

stability field of hydrated basalt than serpentine, but even more because the crust of the subducting plate reheats before the mantle. Likewise, serpentinites in the coolest slab-centre portions of faults may dehydrate deeper within the subduction zone[39]. In North Chile, intraslab earthquakes occur in the ocean crust at 100–150 km depth, and in the slab mantle at depths >150 km (ref. 40). Similarly, double seismic zones elsewhere (New Zealand, Tonga, New Britain, Mariana, NE Japan, Kuril, Kamchatka, Aleutian, Alaska, Gorda Plate, Mexico, northern Chile, central Chile[7,41,42]) have a separation between upper and lower seismogenic planes of 15–30 km, with the lower plane reaching deeper into the subduction zone.

The slab fluid budget, recycling and arc magmatism

Faulting along trenches occurs along most of the world subduction zones as indicated by local swath bathymetry data[21–23] and outer rise earthquakes[15,16]. To evaluate the importance of hydration related to bend-faulting on the global budget of water in subduction zones, we estimate the potential volume of water contained in serpentinized mantle offshore of Nicaragua.

For the calculation we assume that serpentinization occurs along the large faults spaced ~2–3 km in the 25 km closest to the trench (Fig. 4), with vigorous hydration beneath the trench slope occurring for 0.3 Myr at the current convergence rate of ~80 km Myr^{-1}. The diffusion speed of water in unfractured serpentine is ~1 km $Myr^{-1/2}$ (ref. 43), implying a maximum potential for ~30% serpentinization of the uppermost mantle if water is always available along faults and diffuses away from the faults through a 'rind' of serpentinized mantle. Consider that the serpentinization is 3–30% at Moho depths and decreases linearly to 0% at the ~30 km or 600 °C thermal depth limit to serpentinization in ~23-Myr-old lithosphere (the depth where brittle faulting may stop). Chemically bound water forms 13 wt% of serpentine, implying that this 30-km-thick mantle section with 1.5–15% average serpentinization would hold the chemically bound equivalent of a column of 0.17–1.7 km of water per unit length of trench. Previous estimates of 0.14 km (ref. 12)—1 km (ref. 13) for the non-sediment water supplied to subduction zones have generally focused on the water contained in the ocean crust. The above crude estimate for Nicaragua suggests that serpentinized mantle may have the potential to subduct as much chemically bound water as does the oceanic crust.

Additionally, serpentinization may provide a geochemical pathway for recycling water-soluble trace elements into both the sub-arc region of flux-melting and the deeper mantle. Furthermore, sediments are likely to lose more than two-thirds of their chemically bound water by ~50 km depth, and amphibolitized crust (and sediments) will dehydrate almost completely after subducting to ~120 km in typical subduction zone environments[39]. But antigorite serpentine is one of the most stable hydrous phases[44], so that serpentinized lithosphere will progressively dehydrate until the ~200 km depth of the antigorite–phase A hydrous phase transformation[10], at which point dehydration greatly slows or stops.

This implies that antigorite will be the primary source of hydrous fluids from the dewatering slab between 120–200 km depths, potentially providing a key fluid-component to arc-magmas. As these reducing high-temperature fluids migrate upward through the overlying crust and sediments they may be able to scavenge Pb, Be, and similar-behaviour elements from the slab crust, and sediments through which they migrate[39], leading to the preferential hydrous 'leaching' of Pb with respect to Ce that is thought to be linked to the formation of the 'HIMU' mantle source component[45]. Serpentine that transforms to phase A may also recycle a geochemically significant amount of rare gases into the mantle (sea water contains 1%, and 3% of the exosphere's Ar, and Xe, respectively), providing an effective mechanism for this previously hypothesized geochemical process[46].

Thus our observations demonstrate that the oceanic lithosphere undergoes widespread deformation during bending at the MAT. Active faulting across the entire ocean trench slope penetrates at least 20 km into the plate. We infer that faulting provides a mechanism for pervasive infiltration of water into the crust and mantle. This leads to a profound chemical transformation of the lithosphere during which it acquires a series of characteristics that help to explain the generation of intermediate-depth earthquakes and arc magmatism. Although the amount of bend-faulting may change within a few hundred kilometres of distance along a trench, this change is usually linked to locally thickened crust. Oceanic lithosphere rapidly attains much of its thickness during the first ~25 Myr after formation, whereas for older ages thickening slows down considerably. Assuming that the depth of fault penetration is mainly controlled by bending stresses and rheology, we anticipate that similar bend-faulting related processes occur along most subduction zones. □

Received 1 October 2002; accepted 23 July 2003; doi:10.1038/nature01961.

1. Savage, J. C. The mechanics of deep-focus faulting. *Tectonophysics* **8,** 115–127 (1969).
2. Frohlich, C. The nature of deep-focus earthquakes. *Annu. Rev. Earth Planet. Sci.* **17,** 227–254 (1989).
3. Raleigh, C. B. & Paterson, M. S. Experimental deformation of serpentinite and its tectonic implications. *J. Geophys. Res.* **70,** 3965–3985 (1965).
4. Kirby, S., Engdahl, E. R. & Denlinger, R. in *Subduction: Top to Bottom* (eds Bebout, G. E., Scholl, D., Kirby, S. H. & Platt, J. P.) 195–214 (Geophysical Monograph 96, American Geophysical Union, Washington, 1996).
5. Tibi, R., Bock, G. & Estabrook, C. H. Seismic body wave constraint on mechanisms of intermediate-depth earthquakes. *J. Geophys. Res.* **107,** 101029/2001JB000361 (2002).
6. Meade, C. & Jeanloz, R. Deep focus earthquakes and recycling of water into the Earth's mantle. *Science* **252,** 68–72 (1991).
7. Peacock, S. Are the lower planes of double seismic zones caused by serpentine dyhydration in subducting oceanic mantle? *Geology* **29,** 299–302 (2001).
8. Jiao, W., Silver, P. G., Fei, Y. & Prewitt, C. T. Do intermediate- and deep-focus earthquakes occur on preexisting weak zones? An examination of the Tonga subduction zone. *J. Geophys. Res.* **105,** 28125–28138 (2000).
9. Gill, J. *Orogenic Andesites and Plate Tectonics* (Springer, New, 1981).
10. Ulmer, P. & Trommsdorff, V. Serpentine stability to mantle depths and subduction-related magmatism. *Science* **268,** 858–861 (1995).
11. Ernst, W. G. Hornblende. The continent maker—Evolution of H_2O during circum-Pacific subduction versus continental collision. *Geology* **27,** 675–678 (1999).
12. Peacock, S. Fluid processes in subduction zones. *Science* **248,** 329–337 (1990).
13. Moore, J. C. & Vrolijk, P. Fluids in accretionary prisms. *Rev. Geophys.* **30,** 113–135 (1992).
14. Seno, T. & Yamanaka, Y. in *Subduction: Top to Bottom* (eds Bebout, G. E., Scholl, D., Kirby, S. H. & Platt, J. P.) 347–355 (Geophysical Monograph 96, American Geophysical Union, Washington, 1996).
15. Christensen, D. H. & Ruff, L. Seismic coupling and outer rise earthquakes. *J. Geophys. Res.* **93,** 13421–13444 (1988).
16. Hasegawa, A., Horiuchi, S. & Umino, N. Seismic structure of the northeastern Japan convergent margin: A synthesis. *J. Geophys. Res.* **99,** 22295–22311 (1994).
17. Barckhausen, G. A., Ranero, C. R., von Huene, R., Cande, S. & Roeser, H. Revised tectonic boundaries in the Cocos Plate off Costa Rica: Implications for the segmentation of the convergent margin and for plate tectonic models. *J. Geophys. Res.* **106,** 19207–19220 (2001).
18. Protti, M., Guendel, F. & McNally, K. Correlation between the age of the subducting Cocos plate and the geometry of the Wadati-Benioff zone under Nicaragua and Costa Rica. *Geol. Soc. Am. (Spec. Pap.)* **295,** 309–326 (1995).
19. Li, C. Forearc structures and tectonics in the Southern Peru—Northern Chile continental margin. *Mar. Geophys. Res.* **17,** 97–113 (1995).
20. von Huene, R. *et al.* Tectonic control of the subducting Juan Fernández Ridge on the Andean margin near Valparaiso, Chile. *Tectonics* **16,** 474–488 (1997).
21. von Huene, R. & Ranero, C. R. Subduction erosion and basal friction along the sediment starved convergent margin off Antofagasta Chile. *J. Geophys. Res.* **108**(2079), 101029/2001JB001569 (2003).
22. Kobayashi, K., Nakanishi, M., Tamaki, K. & Ogawa, Y. Outer slope faulting associated with the western Kuril and Japan trenches. *Geophys. J. Int.* **134,** 356–372 (1998).
23. Masson, D. G. Fault patterns at outer trench walls. *Mar. Geophys. Res.* **13,** 209–225 (1991).
24. Ranero, C. R., Reston, T. J., Belykh, I. & Gnibidenko, H. Reflective oceanic crust formed at a fast-spreading center in the Pacific. *Geology* **25,** 499–502 (1997).
25. Barth, G. A. & Mutter, J. C. Variability in oceanic crustal thickness and structure: Multichannel seismic reflection results from the northern East Pacific Rise. *J. Geophys. Res.* **101,** 17951–17975 (1996).
26. Detrick, R. S. *et al.* Seismic structure of the southern East Pacific Rise. *Science* **259,** 499–503 (1993).
27. Carbotte, S. M., Solomon, A. & Ponce-Correa, G. Evaluation of morphological indicators of magma supply and segmentation from a seismic reflection study of the East Pacific Rise 15 30'-17 N. *J. Geophys. Res.* **105,** 2737–2759 (2000).
28. Phipps Morgan, J., Harding, A., Orcutt, J., Kent, G. & Chen, Y. J. in *Magmatic Systems* (ed. Ryan, M. P.) 139–178 (Academic, 1994).
29. Morton, J. & Sleep, N. A mid-ocean ridge thermal model: constraints on the volume of axial hydrothermal flux. *J. Geophys. Res.* **90,** 11345–11353 (1985).
30. Nicolas, A. *Structures of Ophiolites and Dynamics of Oceanic Lithosphere* (Kluwer Academic, Dordrecht, 1989).
31. Phipps Morgan, J. & Chen, Y. J. The genesis of oceanic crust: Magma injection, hydrothermal circulation, and crustal flow. *J. Geophys. Res.* **98,** 6283–6297 (1993).

32. Hallenborg, E., Harding, A. J., Kent, G. M. & Wilson, D. S. Seismic structure of 15 Ma oceanic crust formed at an ultra-fast spreading East Pacific Rise: evidence for kilometer-scale fracturing from dipping reflectors. *J. Geophys. Res.* (in the press).
33. Ranero, C. R., Banda, E. & Buhl, P. The crustal structure of the Canary Basin: Accretion processes at slow spreading centers. *J. Geophys. Res.* **102,** 10185–10201 (1997).
34. Carbotte, S. M. & Macdonald, K. C. Comparison of the seafloor tectonic fabric at intermediate, fast, and super fast spreading ridges: Influence on spreading rate, plate motions, and ridge segmentation on fault patterns. *J. Geophys. Res.* **99,** 13609–13631 (1994).
35. Sibson, R. H. Controls on low-stress hydrofracturing dilatancy in thrust, wrench and normal fault terrains. *Nature* **289,** 665–667 (1981).
36. Lynnes, C. S. & Lay, T. Source process of the great 1977 Sumba earthquake. *J. Geophys. Res.* **93,** 13407–13420 (1988).
37. Langseth, M. G. & Silver, E. The Nicoya convergent margin—a region of exceptionally low heat flow. *Geophys. Res. Lett.* **23,** 891–894 (1996).
38. Yamano, M. & Uyeda, S. Heat-floor studies in the Peru trench subduction zone. *Proc. ODP Sci. Res.* **112,** 653–661 (1990).
39. Ruepke, L. H., Phipps Morgan, J., Hort, M. & Connolly, J. A. D. Are the regional variations in Central American arc lavas due to differing basaltic versus peridotitic slab sources of fluids? *Geology* **30,** 1035–1038 (2002).
40. Bock, G., Schurr, B. & Asch, G. High-resolution image of oceanic Moho in the subducting Nazca plate from P-S converted waves. *Geophys. Res. Lett.* **27,** 3929–3932 (2000).
41. Cassidy, J. F. & Waldhauser, F. Evidence for both crustal and mantle earthquakes in the subducting Juan de Fuca plate. *J. Geophys. Res.* **108,** 10101029/2002GL015511 (2003).
42. Hacker, B. R., Peacock, S. M., Abers, G. A. & Holloway, S. D. Subduction factory 2. Are intermediate-depth earthquakes in subducting slabs linked to metamorphic dehydratation reactions? *J. Geophys. Res.* **108,** 20101029/2001JB001129 (2003).
43. Macdonald, H. & Fyfe, W. S. Rate of serpentinization in seafloor environments. *Tectonophysics* **116,** 123–135 (1985).
44. Schmidt, M. W. & Poli, S. Experimentally based water budgets for dehydrating slabs and consequences for arc magma generation. *Earth Planet Sci.* **163,** 361–379 (1998).
45. Chauval, C., Hofmann, A. W. & Vidal, P. HIMU-EM: The French-Polynesian connection. *Earth Planet. Sci. Lett.* **110,** 99–119 (1992).
46. Porcelli, D. & Wasserburg, G. J. Mass transfer of helium, neon, argon, and xenon through a steady-state upper mantle. *Geochim. Cosmochim. Acta* **59,** 4921–4937 (1995).
47. Ranero, C. R. & Von Huene, R. Subduction erosion along the Middle America convergent margin. *Nature* **404,** 748–752 (2000).

Acknowledgements The bathymetry data were collected during R/V *Sonne* cruises 76, 81, 107, 144, 150 and 163, R/V *Meteor* cruise 54 and R/V *M. Ewing* cruises 0005 (Chief Scientist K. McIntosh) and 0104 (Chief Scientist A. Fisher). The seismic reflection data were collected during BGR99 cruise aboard M/V *Professor Polshkov*. We thank the scientific parties for their efforts and officers and crews for their technical and logistical support. R/V *Sonne* cruises were funded by Deutsche BMBF, the R/V *Meteor* cruise by the DFG and the R/V *M. Ewing* cruises by the NSF-USA. This work is a contribution of 'SFB574 Volatiles and Fluids in Subduction Zones' from the University of Kiel.

Competing interests statement The authors declare that they have no competing financial interests.

Correspondence and requests for materials should be addressed to C.R.R. (cranero@geomar.de).